Available online at www.sciencedirect.com

ScienceDirect

Procedia Engineering 213 (2018) 699–707

Procedia Engineering

www.elsevier.com/locate/procedia

7th International Conference on Fatigue Design, Fatigue Design 2017, 29-30 November 2017, Senlis, France

# Sintered steel endurance limit applied to main bearing caps: an innovative probabilistic approach

Jean-Michel Fiard[a]*, Didier Miazga[a]

[a] *RENAULT SAS, Direction de la Mécanique, Guyancourt, France*

**Abstract**

Nowadays, 3D numerical and fatigue analysis have become common place to design parts in the automotive industry. A small investment in numerical simulation often enables to save a lot of time and avoid onerous validation tests. Nevertheless, the major challenge now is to obtain more predictive models. To do so, we need to develop tailored modelling for materials using probabilistic approaches in order to take into account the scatter of physical properties occurring in the manufacturing process or inherent to fatigue mechanisms.
We illustrate here this theme in the context of introducing a new sintered steel material for main bearing caps of recent 3 cylinder gasoline engines. We have developed an innovative experimental and numerical methodology along with a probabilistic approach to determine endurance limit. A four point bending test has been developed and specimens machined from parts have been used to be as close as possible of actual material properties and loadings.
A virtual numerical model of the test bed, tightly correlated with strain measures allowed to calibrate fatigue campaigns and also gave access to mechanical variables of high cycle fatigue tests. Finally probabilistic S-N models have been identified with the "likelihood maximization method" at two stress ratio higher than +0.1. Thus, a resultant fatigue domain related to the part's reliability objective has been defined for the design department.


Peer-review under responsibility of the scientific committee of the 7th International Conference on Fatigue Design.

*Keywords:* fatigue; sintered steel; bearing caps; probabilistic model

* Corresponding author. Tel.: +33-176872341
*E-mail address:* jean-michel.fiard@renault.com

1877-7058 © 2018 The Authors. Published by Elsevier Ltd.
Peer-review under responsibility of the scientific committee of the 7th International Conference on Fatigue Design.
10.1016/j.proeng.2018.02.066

## 1. Introduction

**Nomenclature**

| | |
|---|---|
| A% | strain to failure |
| A | fatigue model parameters |
| B | fatigue model parameters |
| C | fatigue model parameters |
| d | distance between loading rolls |
| E | endurance limit |
| FEA | finite element analysis |
| N | number of cycles to failure |
| Rp0.2 | 0.2% offset yield stress |
| Rm | ultimate tensile stress |
| S | stress |
| S-N | stress versus number of cycle to failure curve |

This article deals with a numerical and experimental combined analysis to estimate the sintered steel endurance limit for main bearing caps. The main bearing caps hold in place the crankshaft in the cylinder block.

Fig. 1 shows an example of bearing caps – with localization of the critical zones - associated with an open deck cylinder block without skirt. Cast iron is the usual choice for bearing caps but for a better compromise between costs, mass and material supply, sintered steel is preferred for a small gasoline engine.

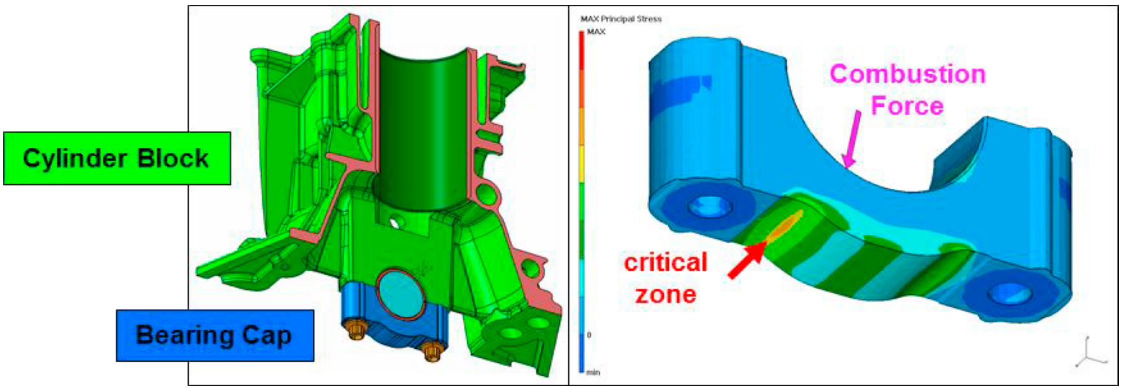


Fig. 1: example of bearing caps

Main bearing caps have to withstand to static and dynamic loads. Static loads are due to main journal mounting, screw clamping and residual stresses. Dynamic loads come from combustion and inertia forces, applied by the piston through the conrod and crankshaft, with a very high number of cycles up to ten millions at maximum load over customer usage. Due to those two kinds of loads we have to design the part to overcome the risk of high cycle fatigue failure at positive load ratio.

The purpose of this article is to present our method to get actual and robust fatigue properties. The main points of this method are firstly to extract specimens from production parts, secondly to use a dedicated test rig with appropriated load conditions and thirdly to apply statistical analysis in order to get a probabilistic fatigue model.

First section is devoted to static measurements. Then we describe the specific test rig and procedure to identify the material behavior. The next section presents the fatigue test campaign and associated statistical analysis. The final result is a new Haigh diagram for FEA with a larger safety domain compared to one deducted from the existing standards.

## 2. Static properties

Monotonic tensile and compressive strength tests have been carried out to identify Rp0.2 and ultimate stress. Young modulus has been identified by vibration in bending mode. Specimens were extracted from real parts for representativeness. The Table 1 shows slight differences between FC-0208-50 standard ((a) column) of Metal Powder Industries Federation (cf. [1]) and our experimental results ((b) column).

Table 1: Rp0.2, ultimate stress and Young modulus

| Property (unit) | (a) Standard | (b) In-house Tests | (c) Test - Standard |
|---|---|---|---|
| E(GPA) | 120 | 140 | +17% |
| $Rp_{0.2}$(MPa) | 380 | 339 | -11% |
| Rm (MPa) | 410 | 434 | +6% |
| A (%) | <1.0 | 1.1 | |

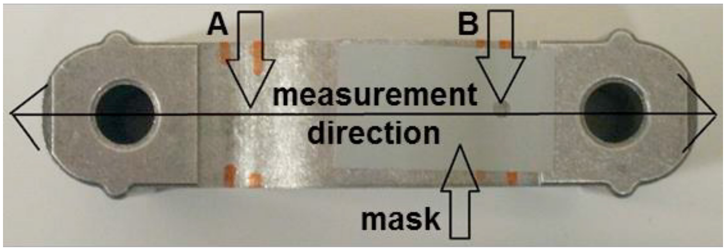


Fig. 2: measurement locations (A and B) for residual stresses

Table 2: statistical results of residual stresses

| MPa | A | B |
|---|---|---|
| Mean value | -178 | -175 |
| Standard deviation | 27.6 | 31.7 |

Sintered manufacturing process leads to surface residual stresses which were measured on enough parts to allow a statistic analysis. We measured residual stresses on the two critical zones (cf. Fig. 2) by X ray diffraction. The results summarized on and Table 2 indicate significant compressive stresses that should have a positive impact on fatigue limit.

Note: density scatterings have been measured too, in order to check the conformity of the parts relative to standard.

## 3. Bearing caps test rig

In order to be as close as possible to service conditions in the critical zones a four point bending test rig has been used with specific specimens.

Four point bending tests allow to have a constant bending moment in the critical area. The specimen are machined from production parts in order to remove the upper part and get a flat surface as shown on the Fig. 3.

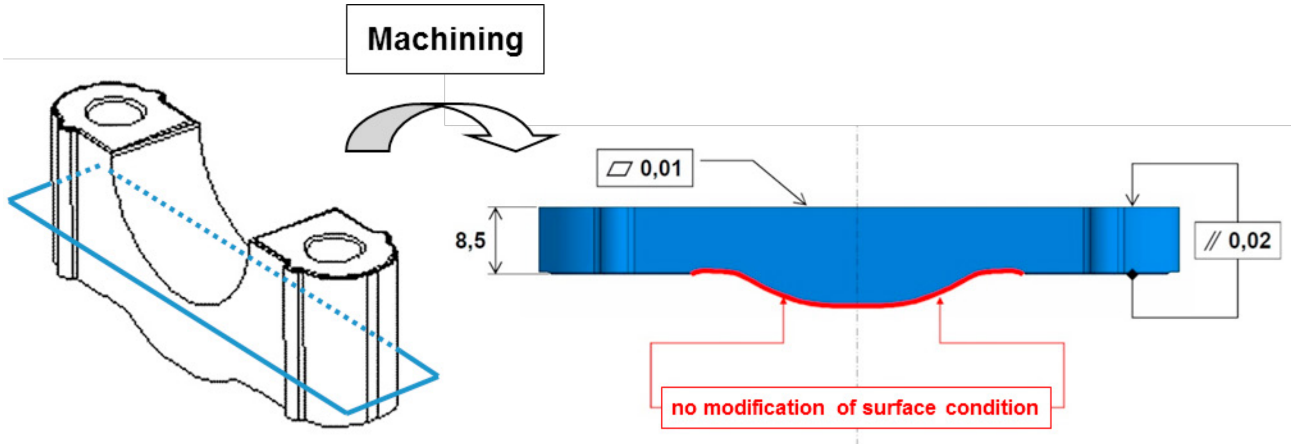


Fig. 3: specimen description

Load is applied by means of two loading rolls and reaction forces are done by two supporting rolls (cf. Fig. 4). Distances between loading (d) and supporting rolls (D) are adjusted in order to have the higher stresses in the critical zones.

This test rig have been used for static and dynamic tests; the first one for correlation with simulation and the second one to get Wohler curves.

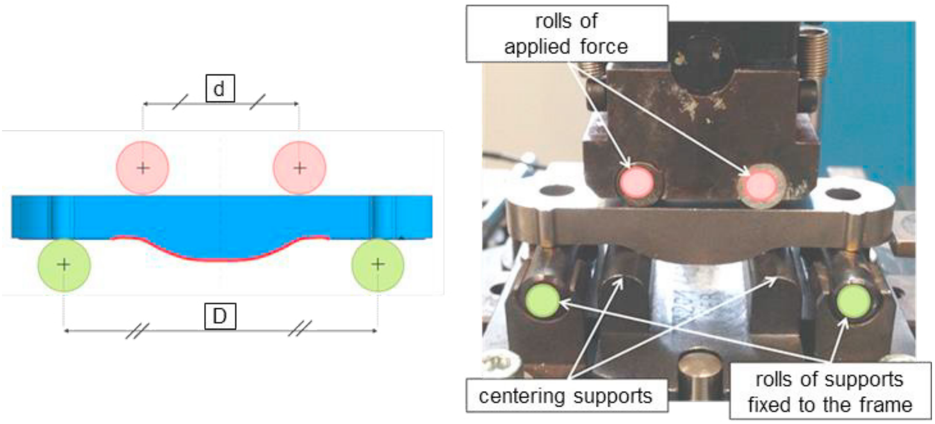


Fig. 4: test rig description

## 4. Numerical model of test rig

A numerical model have been developed (cf. Fig. 5) with second order tetrahedron finite elements (Abaqus C3D10 element) for a quarter of specimen to take advantage of symmetries and with rigid surfaces for cylinders. One can check on Fig. 5 the similarities between stress state between test rig and engine running test.

Linear elastic behavior has been chosen for specimens. This revealed to be appropriate to this material. Thus, The numerical model has four parameters to be adjusted;

- the Young modulus and the Poisson coefficient that define the material behavior,
- the friction coefficient at the interface between cylinders and specimens,

- the distance between loading rolls (d).

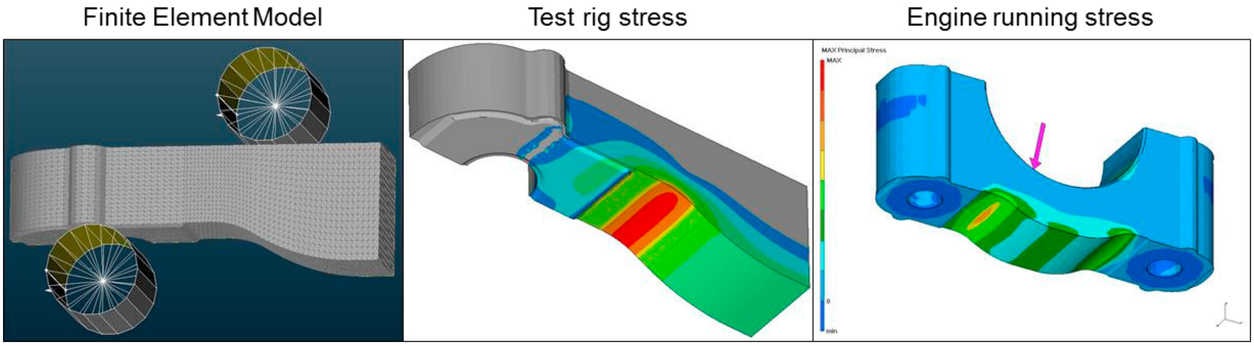


Fig. 5: Numerical model of test rig

To calibrate the model, strain gauges have been placed on a specimen: two on the sides, two on the top and two on the bottom. Position sensor has been used too as shown on Fig. 6

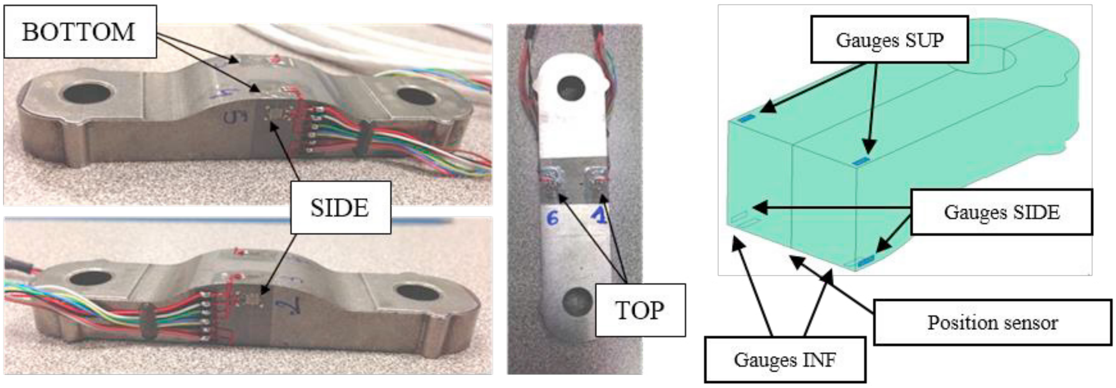


Fig. 6: location of strain gauges and position sensor

After preliminary monotonic increasing loads on ordinary sample to evaluate the resistance of the structure we apply the program depicted on Fig. 7a on the instrumented specimen. We observe linear response of the structure on Fig. 7b for 7 and 8 kN loads. The Fig. 8 gives the response function of loads and we notice no plastic strain until 11 kN load which justifies to use linear elastic material law.

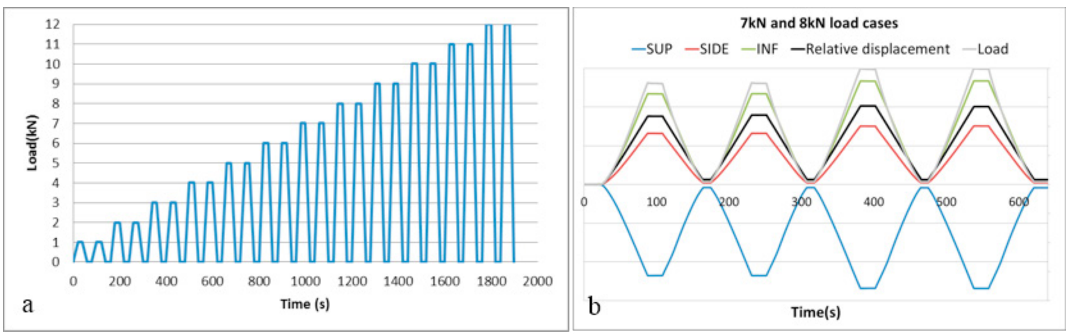


Fig. 7: a) test program, b) 7 and 8 kN detailed strain results

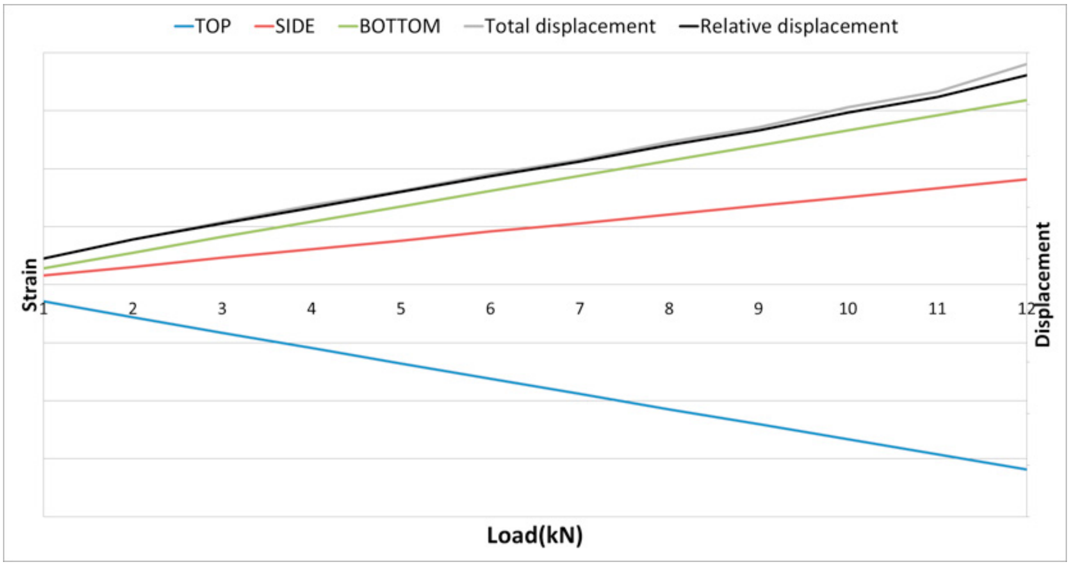


Fig. 8: measured strains function of loads

A design of experiment has been done to identify the better set of model parameters defined previously. Poisson coefficient is fixed to avoid infinite number of solutions. Variation domains are respectively [100GPa, 170GPa], [9mm, 15mm] and [0%, 3%] for Young modulus, distance between loading rolls, friction coefficient. Notice that thanks to the very low tolerance on geometry due to process, the part geometry is close to nominal and does not need to vary. The objective is to find the set of parameters that reduces as much as possible the gap between strains measured and strains computed on the six locations.

A lot of configurations has been tested to cover parameter variation domain (simulation cost is low). Partial results presented on Fig. 9 illustrate the sensitiveness of the model response to the parameters. In the end, the best set of parameters is given by the measurement of Young modulus done by the Renault's Material department, the nominal distance on drawing between loading rolls and a low friction coefficient of 0.05. With this set of parameters the disparity between measures and simulation is less than 3% as depicted on Fig. 9.

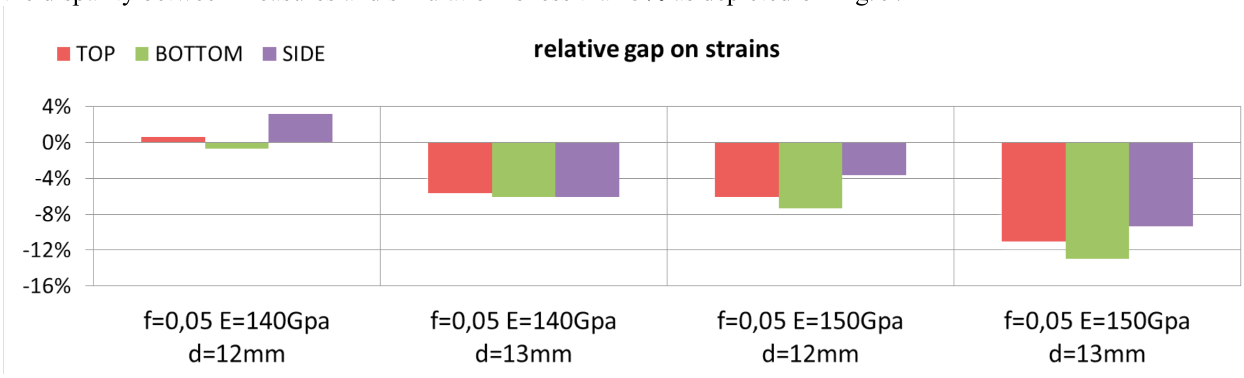


Fig. 9: simulation versus measures

This satisfactory correlation – in concordance with measures - is also due to the low geometric scatterings thanks to the tight tolerance allowed with the sintered process. Notice that this point is very different from the cast iron process where the geometric dispersion is very high.

## 5. Fatigue experiment procedure and analysis

Fatigue tests at ambient temperature have been performed on Roell Amsler dynamic testing machine in the following conditions:

- 60Hz frequency,
- Ambient temperature,
- 2 load ratio $R=F_{min}/F_{max}$.; R=+0.12 and R=0.22,
- 5 samples at each level.

Raw results are presented on Fig. 10 where input and actual values correspond respectively to the programmed values and the real measured values.

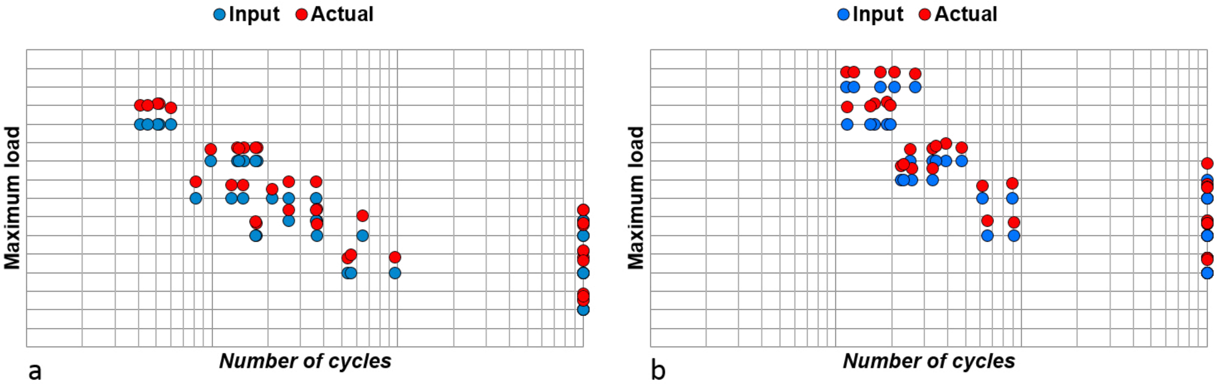


Fig. 10: raw fatigue results; (a) R=+0.12, (b) R=+0.22

Force-to-stress conversion in the critical area is given by the numerical model.

For Fatigue curves we used Stromeyer model $N = A/(S - E)$) that gives the number of cycles $N$ function of the level of stress $S$ and the fatigue limit $E$. $A$ is the slope in the $(1/N;S)$ diagram. We assume that fatigue limit is a random variable with a normal distribution $N(\mu, \sigma^2)$. The mean value is given by Stromeyer model $\mu = S - A/N$ . $E, A, \sigma$ are determined by applying the method of maximum likelihood that consists in maximizing likelihood function $\mathrm{L}$ defined as following:

$$\mathrm{L}(\mathrm{A},\mathrm{E},\sigma) = \prod_{i=1}^{n_{exp}} \mathrm{L}_i(\mathrm{A},\mathrm{E},\sigma)$$

$$\mathrm{L}_i(\mathrm{A},\mathrm{E},\sigma) = \frac{1}{\sigma\sqrt{2\pi}} \exp\left(-\frac{1}{2}\left(\frac{E_i - E}{\sigma}\right)^2\right) \text{ for broken samples}$$

$$\mathrm{L}_i(\mathrm{A},\mathrm{E},\sigma) = \int_{E_i}^{+\infty} \frac{1}{\sigma\sqrt{2\pi}} \exp\left(-\frac{1}{2}\left(\frac{t - E}{\sigma}\right)^2\right) dt \text{ for unbroken samples}$$

$$E_i = S_i - \frac{A}{N_i}$$

The Fig. 11 presents Wohler curves (cf. [2]) given by the identification with the quantiles 10%, 50%, and 90% for respectively the red, blue and green curves.

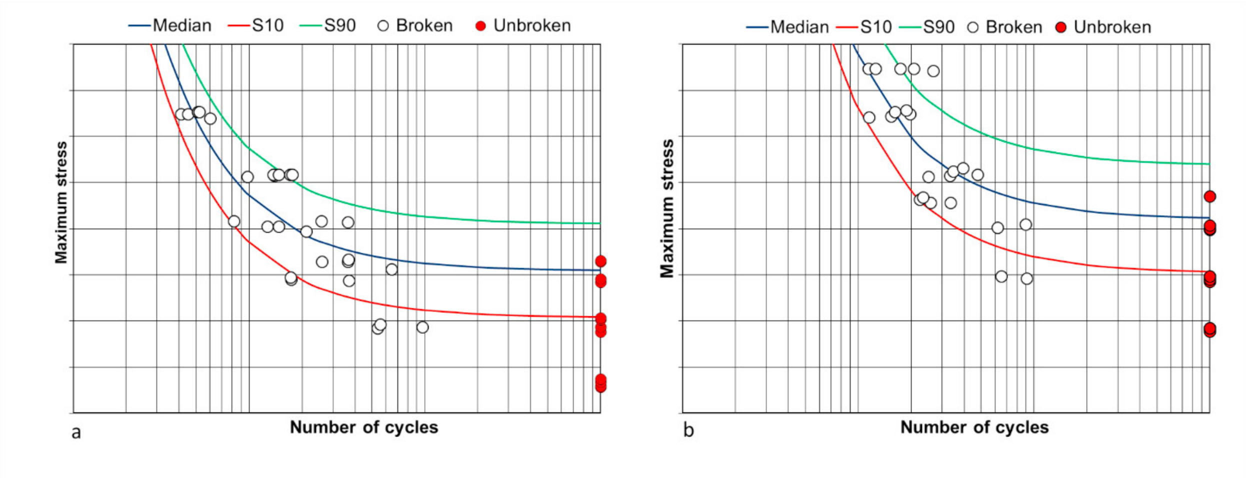


Fig. 11: Wohler curves; (a) R=+0.12, (b) R=+0.22

Remarks:

- Simple linear regression allows to identify parameters of the Stromeyer model and to estimate the associated standard deviation. This method takes only into account broken samples and consequently the model is pessimistic.
- Quantile-quantile diagram (so called "droite de Henry" in French) is not appropriate because we do not have enough results by load level.
- Bastenaire [3] models ($N = (A \cdot \exp(-((S-E)/B)^C)/(S-E))$ ) instead of Stromeyer model along with the method of maximum likelihood gave similar results. Nevertheless Bastenaire model needs more parameters and thus is less relevant according to BIC criteria (Bayesian Information Criteria).

## 6. Haigh diagram

Haigh diagram is relevant for this part because the stress state is mainly uniaxial.

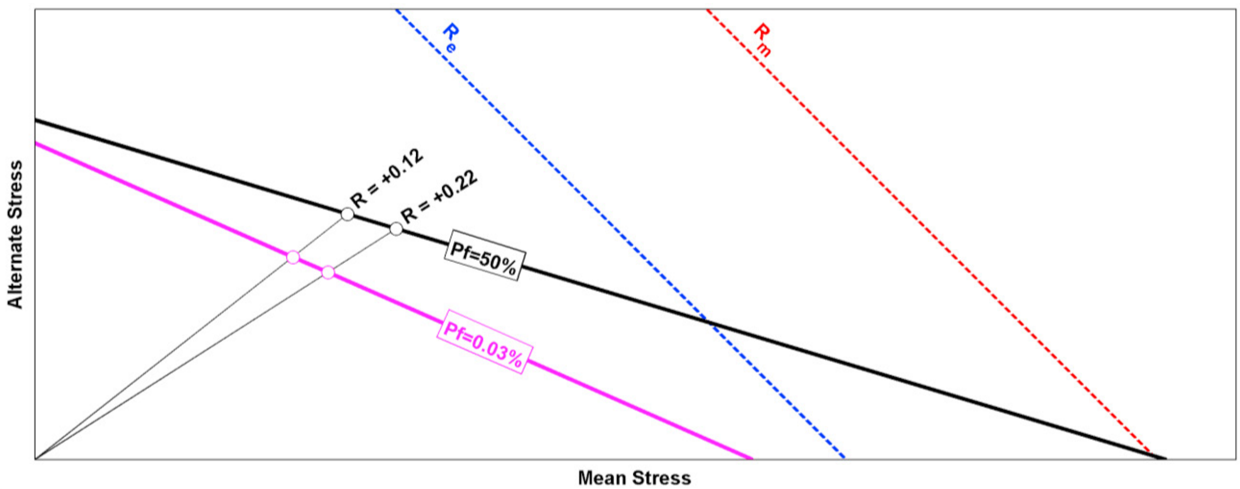


Fig. 12: Haigh diagram

The probabilistic fatigue model provides for a given probability of failure a fatigue limit for each load ratio. The safety domain in Haigh diagram is defined by joining the two corresponding points.

Example is given in the above figure for Probability of failure (Pf) =50% and Pf=0.03%. The Re and Rm line close the domain and are defined by the computed stress associated to the respectively elastic limit and ultimate measured load.

Notice that the domain built only from information available from the standard [1] and with methods available in [4] is very conservative compared to the domain given by our approach and would lead to largely oversizing the part.

## 7. Conclusion

In this study we have taken advantage of a combined experimental-numerical approach. A key point was to build an appropriate four point bending test rig that allows to reproduce stress state in the part during service.

To be representative as much as possible of real part, it was crucial to make specimens from productions parts.

Finally, we developed a numerical approach based on simple principles – easy to understand and to deploy – that leads to the right sizing of the part.

## Acknowledgement

The authors gratefully acknowledge their students Benoit Dauverchain and Kailin Zhu for their fruitfully contribution.

We would like to thank our colleagues Damien Arnal, Thierry Cembrzynski, Nicolas Forissier, Denis Millet, Olivier Salmon and Jean-Claude Vidal for their support.

## References

[1] MPIF Standard 35, Materials Standard P/M Structural Parts, Material Powder Industries Federation, 2000.

[2] J.-L. Chaboche and J. Lemaître, Mécanique des matériaux solides, , 3ème édition, Dunod, 2009.

[3] F. Bastenaire, ASTM Special Techn. Publ. N°511, 1972.

[4] VDI 2226, Empfehlung für die Festigkeitsberechnung metallischer Bauteile, 1965.